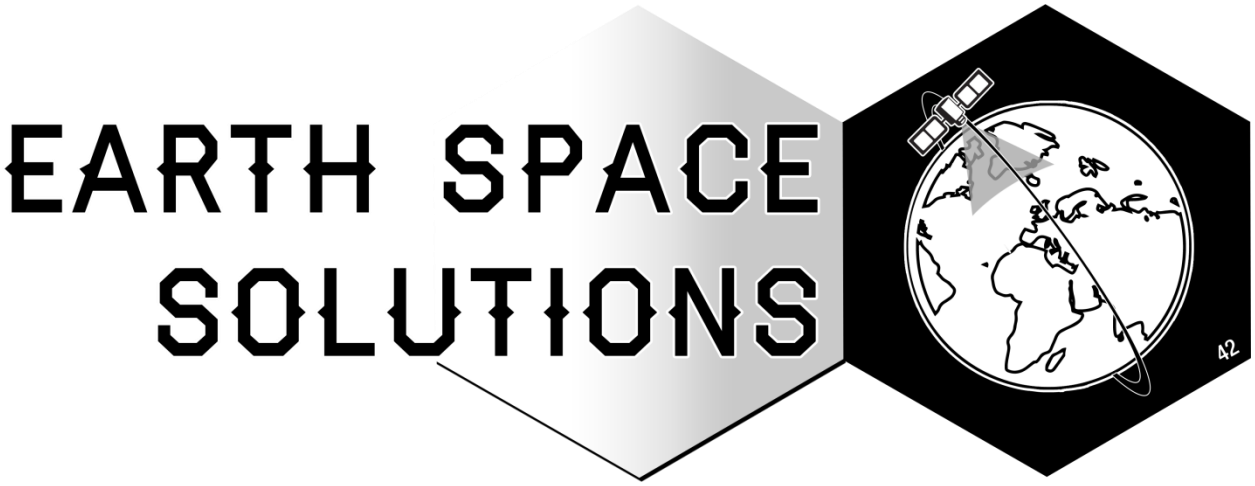

Report

Development of an alternative hyperspectral moon phase reddening model

Prepared by:
Earth Space Solutions (Dr. Matthijs Krijger), Utrecht, The Netherlands

Address:
Earth Space Solutions
Saffierlaan 87
3523RB Utrecht
The Netherlands

Contact:
Dr. Matthijs Krijger
Phone: +31 6 36014769
E-Mail: Krijger@earthspace.nl

Document number:
ESS-AMM-RP-001-Rev5
Version: 2019-10-10

Distribution:
EUMETSAT
Earth Space Solutions

1 CONTENTS

2 EXECUTIVE SUMMARY

In this report we present an updated lunar reflectance model named LESSSR (Lunar ESS SCIAMACHY RELAB), validated by GOME2 and SEVIRI measurements. The model employs a combination of in-flight SCIAMACHY measurements and on ground RELAB measurements and improves on previous (SCIAMACHY) lunar models (due to inclusion of polarization and noise reduction) and GIRO (which shows phase dependence on SWIR wavelengths when compared to other measurements).

3 INTRODUCTION

This document describes a study on the characterisation of the reddening effect on the lunar reflectance spectrum of varying illumination conditions and the comparison with the current GIRO mechanism accounting for this effect.
A model is developed using both data available from the NASA Reflectance Experiment Laboratory and the SCIAMACHY lunar observation. This activity is meant to contribute to the enhancement of the GSICS Implementation of the ROLO (GIRO) model (see http://gsics.atmos.umd.edu/bin/view/Development/LunarWorkArea). The outcome of this study allows a better understanding of the phase dependence observed with some satellite datasets, such as the Meteosat lunar data acquired with the SEVIRI instruments, which cover GIRO's full range of illumination conditions.

4 OBJECTIVES

This section has been copied from the Statement of Work

3.1.1 Noise reduction in SCIAMACHY short wave infrared (Phase A)

Req 1. The possibility to remove or reduce the impact of the residual polarisation in the SCIAMACHY lunar observation dataset shall be investigated.

Req 2. The possibility to reduce the noise in the measurements beyond 1.3 microns shall be investigated.

Req 3. The impact on the SCIAMACHY data of reducing the polarisation and noise artefacts shall be assessed.

Req 4. The mechanism implemented to remove or reduce the residual polarisation artefacts and to reduce the noise in the SCIAMACHY lunar observations shall be described in a comprehensive manner in a Technical Memorandum.

Req 5. The impact assessment of the corrections shall be fully documented.

Req 6. The newly derived SCIAMACHY lunar dataset shall be delivered, together with all the ancillary datasets used to derive it.

3.1.2 Inference of a lunar soil reflectance spectrum as a function of the illumination conditions (Phase B)

Req 7. A model for the lunar soil reflectance spectrum as a function of the phase shall be inferred using data from RELAB data and SCIAMACHY (after applying the corrections from Phase A). This model could be either a parametrisation or a look-up table. The model shall have a spectral resolution at least equivalent to the current Apollo spectrum in the GIRO model (10nm). It is expected that the spectral resolution will be actually much higher.

Req 8. The contractor shall investigate the validity of the model below 350nm using the same data.

Req 9. An assessment of the associated uncertainties using an independent subset of SCIAMACHY spectra shall be provided with the model developed in Req 7.

Req 10. The model newly derived (parametrisation or look-up table) shall be delivered.

Req 11. The prototyping code, used for the model derivation, shall be delivered.

3.1.3 Validation of the reddening effect model and impact assessment (Phase C)

Req 12. The lunar soil reflectance spectrum model inferred in Phase B shall be validated Using the GOME-2 lunar spectra. Additionally, the contractor may propose to use other datasets known to her/him, after documenting adequately the quality of those datasets.

Req 13. An assessment of the impact of changing the current reddening mechanism as implemented in the GIRO shall be performed for the newly derived lunar reflectance model, using the GIRO output for the SEVIRI lunar observations.

Req 14. The Source Code used for the analysis and the representation of the results shall be delivered.

4.1 DELIVERABLES

This section has been copied from the Statement of Work , with WP numbers added.

[D.1] Improved SCIAMACHY dataset (Phase A) [Req 6]

[D.2] Technical Report on Phase A, B and C with the details of the task execution (methodology, results, analysis, etc.) [Req 5] (This report)

[D.3] Moon reddening model (code/script/ancillary data) as inferred for Phase B. [Req 10]

[D.4] Prototype Source Code. [Req 11] and [Req 14]

5 PHASE A: SCIAMACHY IMPROVEMENTS

5.1 SCIAMACHY MEASUREMENTS

In a previous study "the Validation of Spectral Band Adjustment Factors using Lunar Hyperspectral Measurements" [RD-2], over a thousand SCIAMACHY lunar hyperspectral observations were processed. The outcome of this work is employed as a starting point for the present study.
The delivered datasets were retrieved, read in, and checked for (reading) errors.
For later comparison with GOME2 the SCIAMACHY dataset was converted to contain the same information as the GOME2 dataset while retaining SCIAMACHY unique information. Any missing information (such as solar lunar longitude) was extracted from the original GIRO dataset (calculated for the previous study). Measurements were converted to physical units were possible, for easier analyses and comparisons. The dataset was pruned for known erroneous lunar measurements (mispointing by SCIAMACHY), resulting in 1133 lunar measurements. Extensive verification of all information was performed.

Some initial verification with GOME-2 and GIRO-datasets was performed. GOME2 observes the moon at similar absolute phase, but at (mostly) opposite sign. Possibly more important GOME2 observes the moon at very different times when the solar longitude on the moon (sol selen lon) is very different. Phase and Solar Longitude are also coupled, which explains why SCIAMACHY (and GOME2) did not need a solar longitude dependence, as it observed mostly one side of the phase range and could thus describe the solar longitude dependence with the phase dependence. Deriving a new SCIAMACHY (and/or GOME2) model which includes the Solar longitude dependence was not foreseen, but was investigated (and implemented).

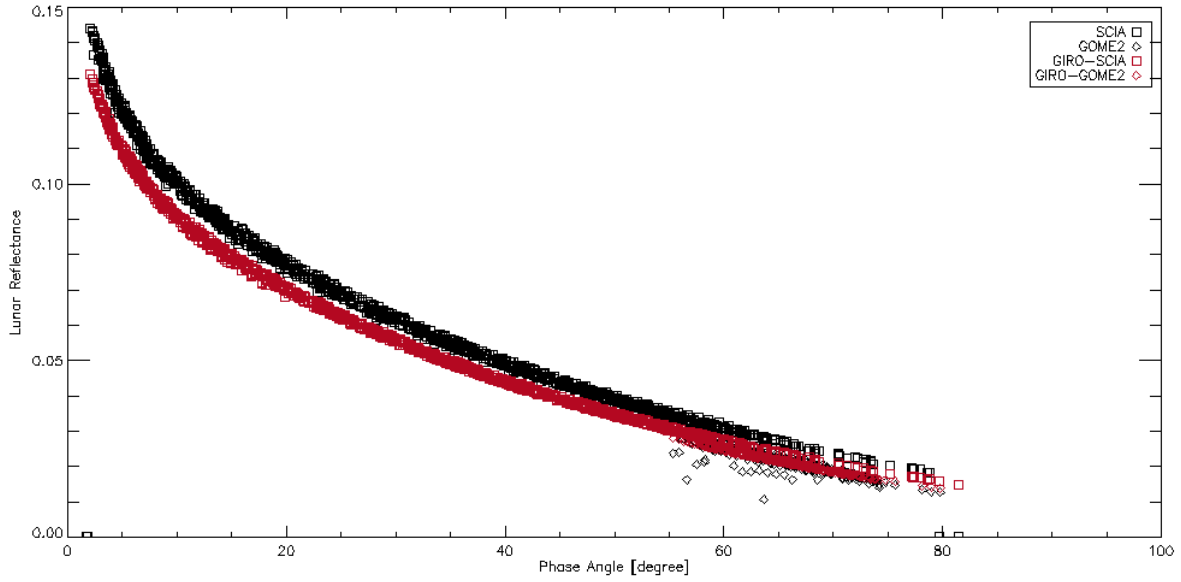

Figure 1 SCIAMACHY Lunar Reflectance as function of absolute phase

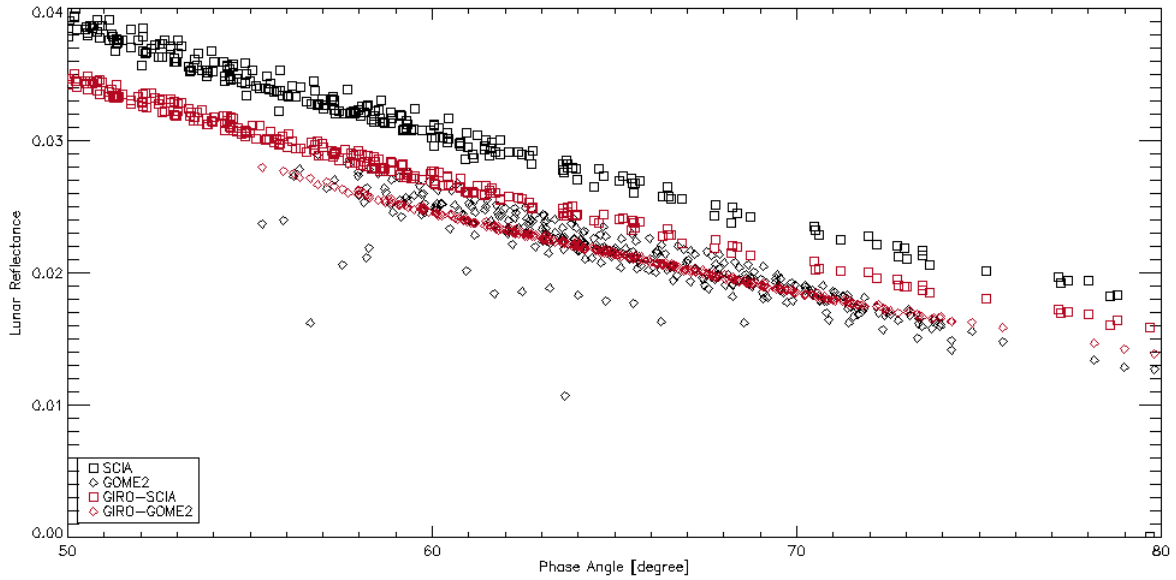

Figure 2 SCIAMACHY Lunar Reflectance as function of absolute phase (zoomed in GOME2 range)

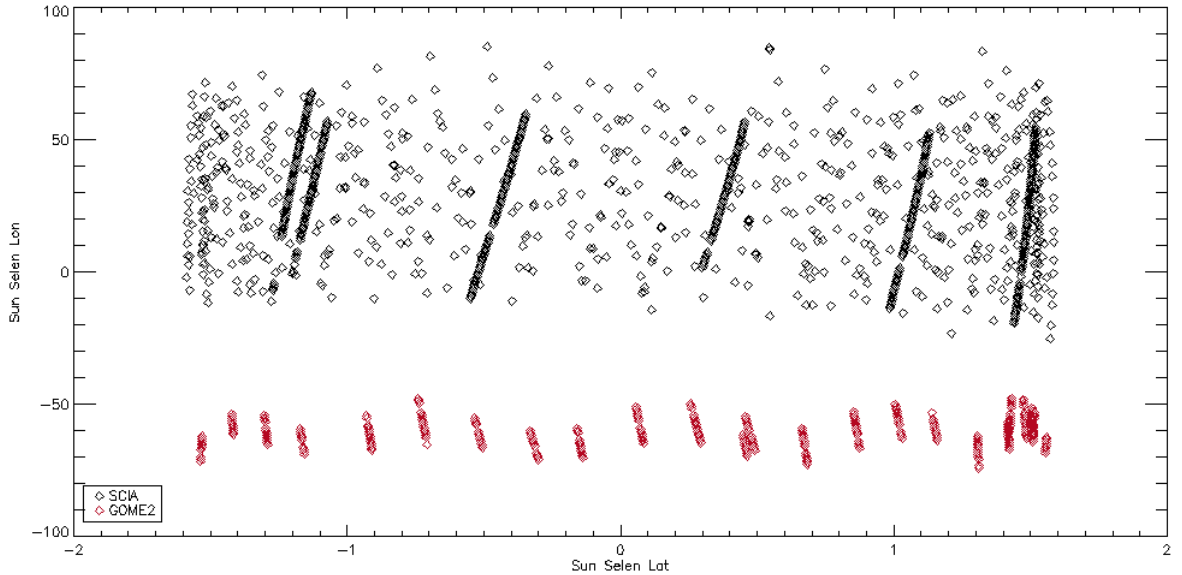

Figure 3 Solar geometries observed

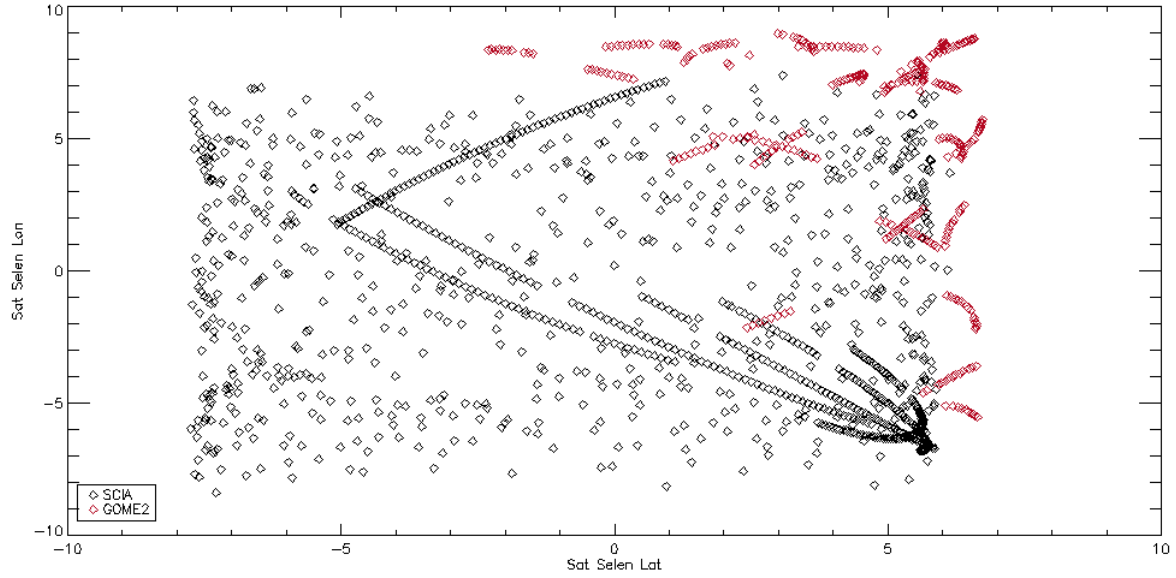

Figure 4 Lunar Libration angles observed

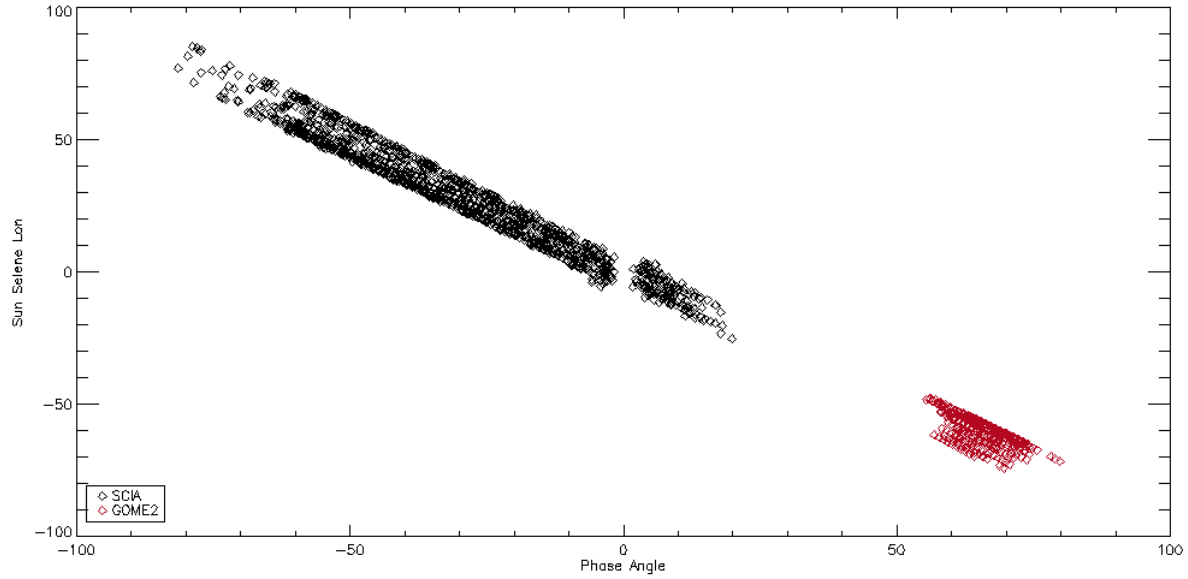

Figure 5 Phase angle as function of solar lunar longitude

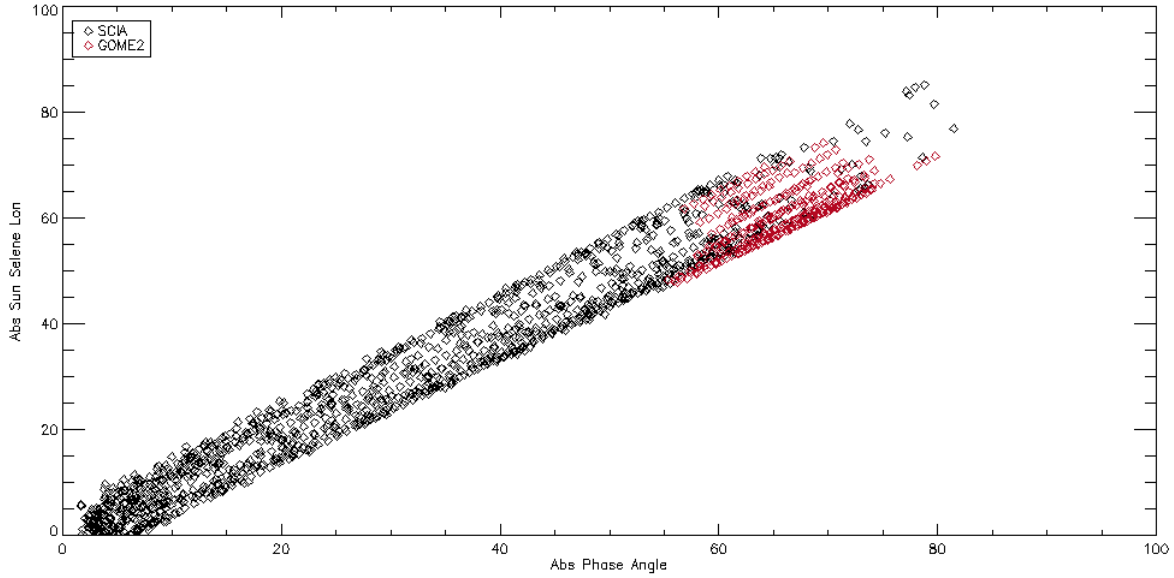

Figure 6 Absolute Phase angle as function of solar lunar longitude

5.2 IMPROVED BRDF CORRECTION

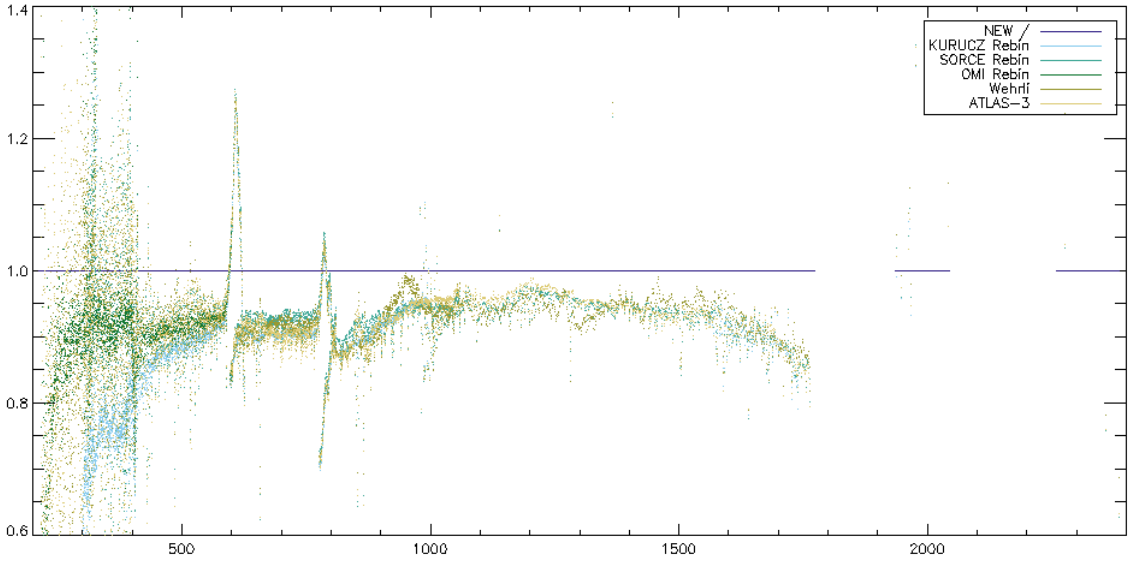

Figure 7 Comparison employed SCIAMACHY solar spectrum with various reference spectra

The SCIAMACHY solar spectra is known to have non-perfect calibration. This is most likely caused by the BRDF correction from the diffuser, meaning that this also affects any (lunar) reflectance. The SCIAMACHY solar spectra is compared to various other (reference) solar spectra and is consistently too low (which likely explains why SCIAMACHY lunar reflectances are consistently higher than GIRO), due to the (unaccurate) distance of the calibration lamp during onground calibration.

Recent investigation into the SCIAMACHY solar spectrum (Hilbig 2018) provided updated improved SCIAMACHY calibration, mostly notable the Bi-direction Reflectance Distribution function (BRDF) which impacts the ratio between lunar and solar irradiance and thus the lunar reflectance for Channel 1, 7 and 8 (UV and NIR/SWIR). The update in absolute radiometric calibration of the solar and lunar irradiance is not relevant here, as the absolute radiometric calibration is divided out in the reflectance. The absolute value of the lunar reflectance is this linearly dependent on the BRDF. While the normal BRDF is geometry dependent, the update

has retained the same geometry dependence and only the initial stable value has changed (BRDF(t,Θ) = BRDF(t_0) * BRDF(Θ)). As such the employed BRDF during the previous study was divided out and the update BRDF divided in.

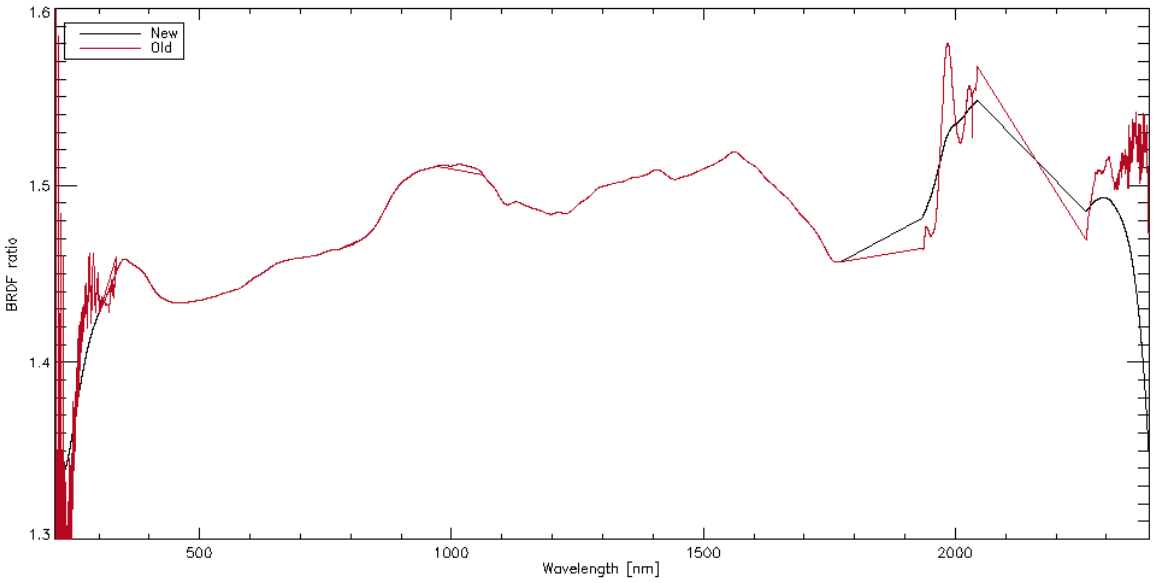

At this stage an (wavelength independent) offset in absolute calibration remains (likely due to an error in the assumed distance of the light source during on ground calibration). After investigation and in discussion with Hildig a wavelength independent correction of 15% was added the SCIAMACHY solar irradiance employed in the previous study (v8b) to match the latest SCIAMACHY calibration results (v9).

5.3 NOISE CORRECTION

The latest version of the SCIAMACHY Dead and Bad pixel map was obtained (version 7.4.2012, IUP Bremen) and applied to the measurements, removing many of the noisy (due to untrustworthy dark correction) pixels. Also the overlap regions between channels were removed as these suffer from various calibration issues. Some pixels that are clearly behaving different from other pixels (noisy pixels) remain in the NIR/SWIR region. This is due to the higher readout noise in these regions and unavoidable. However in later steps in this study, these noisy pixels are identified, flagged and excluded from influencing model fits. Later steps with RELAB spectra also removes these noisy pixels (see those sections).

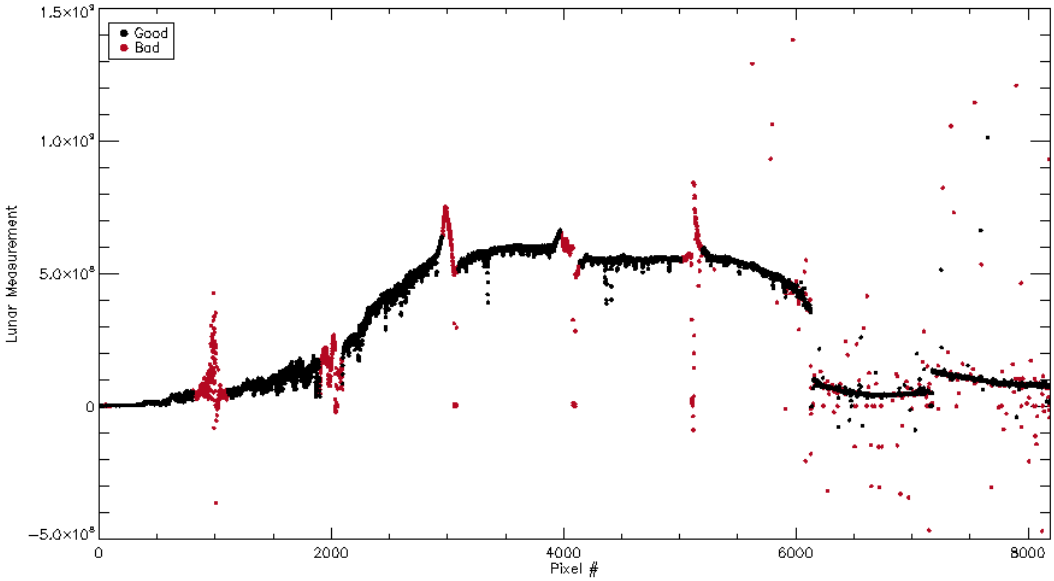

Figure 8 SCIAMACHY lunar measurement with bad pixels indicated

5.4 POLARISATION

5.4.1 SCIAMACHY POLARISATION

SCIAMACHY is sensitive to the polarization of the incident radiation, relative to the entrance slit. During onground calibration it was detected that SCIAMACHY was not only sensitive to polarization ratio between perpendicalar and parallel polarization to slit (Q-polarisation), but unexpectedly also to polarization 45° rotated relative to slit (U-polarisation). Additional measurements were performed to determine this Q and U polarisation sensitivity for all wavelengths (shown in Figure 9). This sensitivity is scan-angle (mirror position) dependent. The polarization itself is measured with 7 broadband onboard Polarisation Measurement Devices (PMDs) and together with polarization single-scattering model values (for low wavelengths) interpolated across wavelength. The combination of (in-flight derived) polarization and (on-ground derived) polarization-sensitivity allows a correction in the Lv0 to Lv1B processor for the measured radiance. In the original study no polarization correction was applied, as the polarization correction was lacking, and broad-band polarization could be mostly removed by modelling an instrumental Azimuth Scan Mirror (ASM) scan angle dependence, but was shown to be coupled with the phase dependence. As such an investigation was performed to improve the polarization correction.

As can be seen in Figure 9 around 350 nm a strong wavelength-structured 80% sensitivity exists to Q-polarisation, hence this feature is often referred to as ‘the’ polarization-feature. When examining all SCIAMACHY measurements, after removing instrumental effects (determined in the previous study: Validation of Spectral Band Adjustment Factors using Lunar Hyperspectral Measurements, Activity 1 & 2, 07.06.2017, ESS-LUN-RP-001-Rev4) for these wavelengths, as shown in Figure 10, a feature is still visible around 350nm impacting reflectance in order of 10%. Such a feature we know from RELAB does not exist in the lunar sample reflectances and is thus most likely non-perfect removed polarization-sensitivity of SCIAMACHY. Recent studies indeed confirmed that the SCIAMACHY polarization correction is lacking (Liebing, et al 2018) due to imperfect polarization determination. The 350nm feature is due to spatially limited damage/contamination of the physical pixels, while the polarization sensitivity is determined with fully illuminated pixels and the lunar measurements only partially illuminate the slit and thus pixels. The feature at 350nm however can be easily corrected for as its spectral structure is easily detected, remaining polarization at other wavelengths is harder to detect and thus correct for. Polarisation is not constant over wavelength and must thus for each wavelength be determined (or interpolated) before correction, assuming the (improved) on-ground sensitivities are still

correct. There are indications that the polarization-sensitivity is also changing over time, but that is outside the scope of this study. To determine lunar polarization for the whole SCIAMACHY wavelength range, it would have been perfect to employ SCIAMACHY own PMDs, but as mentioned the polarization derived from these is not adequate. GOME2 polarisation is much better, but is limited to the small geometries GOME2 observes the moon and thus not applicable for SCIAMACHY. No known measurements exists for all SCIAMACHY wavelengths AND all observed lunar geometries (even if limiting just to lunar phase). (see section 5.4.2). Therefor a model needs be derived.

The Umov-law (which indicates that polarization decreases as radiance increases for (surfaces similar to the moon) suggests that polarization amplitude for higher wavelengths will be lower due the redness of the moon. The polarization correction error is strongly coupled to the polarization amplitude and thus will be lower for higher wavelengths. This is confirmed by investigating other spectral polarization structures such as those around 940-1050nm, as in Figure 11. However the amplitude of this feature is also much smaller and thus less indicative of an polarization correction error, but polarization error on the reflectance seems to be less than 1e-3.

Note that channel overlaps suffer from their own issues and can thus not be employed for polarization investigations (as determined by Tilstra&Krijger in 2003, internal communication).

In Figure 12 and Figure 13 are shown density plots of all expected Q and U sensitivities of SCIAMACHY for all observed geometries. As expected the Q-sensitivity does not vary much as this sensitivity variation comes from Elevation Scan Mirror (ESM) rotation and this mirror rotation is mostly fixed in order to observe the ASM mirror (which is of course fixed inside the instrument). The U-sensitivity varies much more due to the ASM mirror rotation required in order to observe the moon at various locations outside the instrument.

V-polarisation can be ignored (<0.001% (Lipsy and Pospergelis, 1967). Any polarization correction could thus employ only Q-polarisation and U-polarisation. As the exact rotation of SCIAMACHY to the plane of incidence is not known, this rotation must be empirically determined (aka fitted).

SCIAMACHY polarization correction (or function) is described for each wavelength as:

$$1+q * mu2 + u * mu3,$$

with q, and the relative fractional polarization and mu2 and mu3 the polarization sensitivity of SCIAMACHY. The polarization sensitivities for each geometry and wavelength can be derived from the SCIAMACHY mirror model (Krijger et al 2014), while the polarization must be modelled (next section).

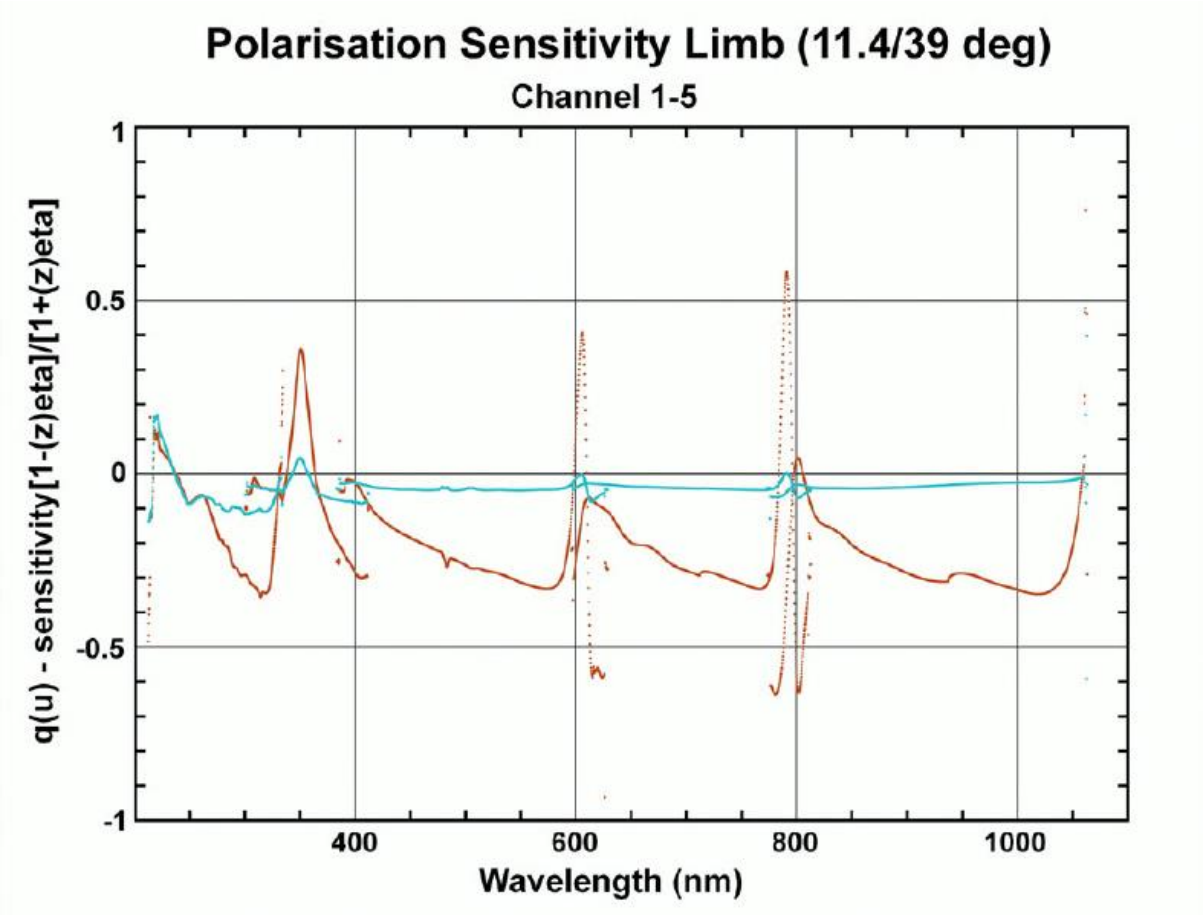

Figure 9 Example SCIAMACHY Polarisation sensitivity (Red -Q, Blue -U) [Taken from SCIAMACHY Handbook]

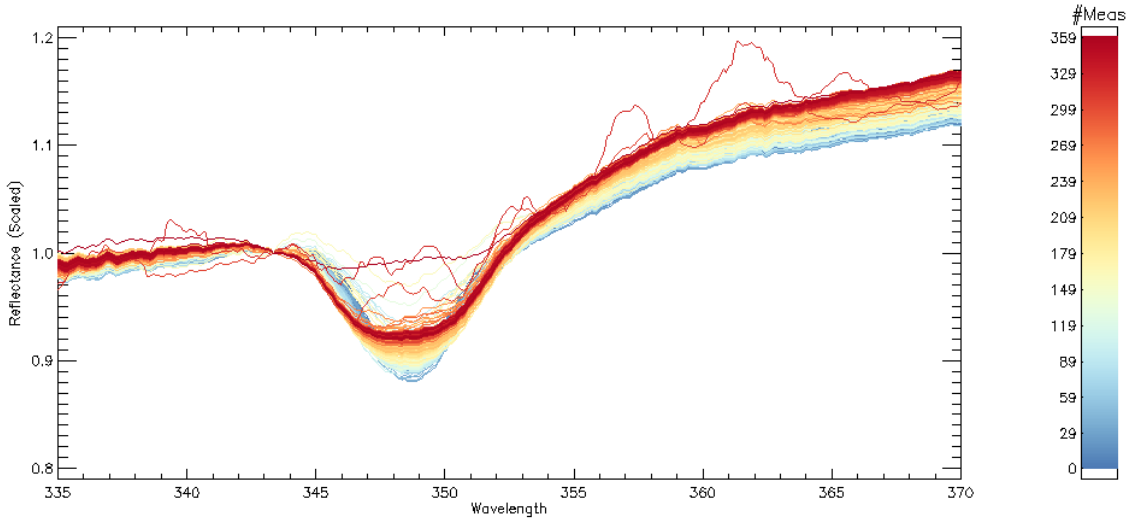

Figure 10 SCIAMACHY lunar reflectance (with instrument effects removed), scaled to 343nm

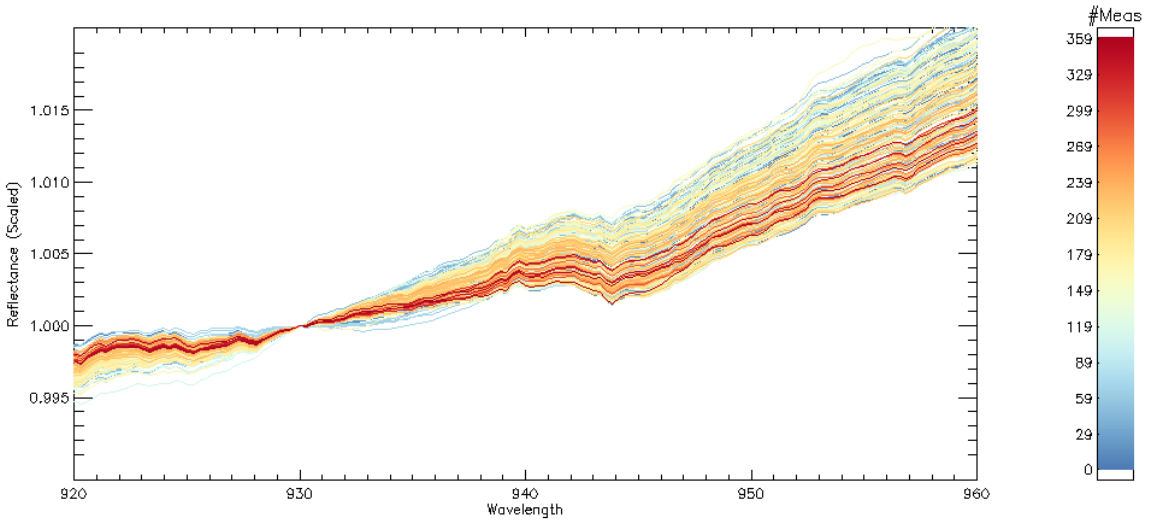

Figure 11 SCIAMACHY lunar reflectance (with instrument effects removed), scaled to 930nm

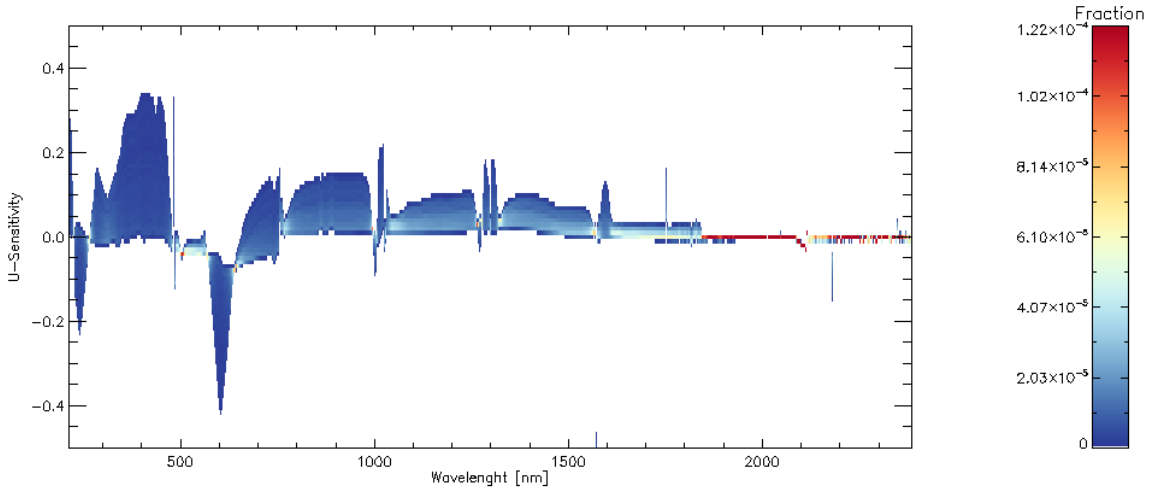

Figure 12 Density plot of the expected U-sensitivity for all observed geometries

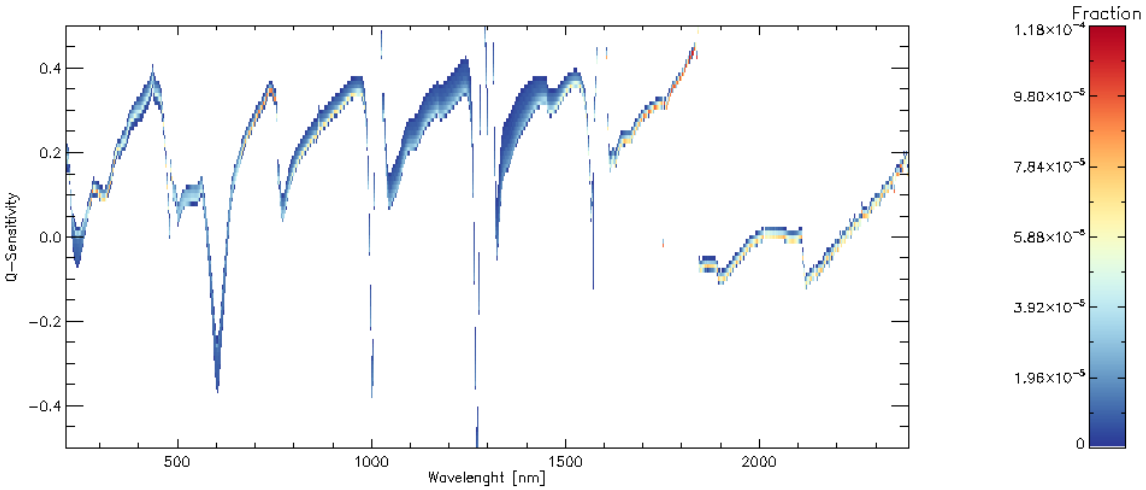

Figure 13 Density plot of the expected Q-sensitivity for all observed geometries

5.4.2 LITERATURE STUDY

An extensive literature study was performed (references in Reference section), investigating lunar polarization models. But to quote Shkuratov et al. (2017): "Although lunar polarimetry has a long history, it has not been a popular topic". No polarization model of the moon exists, and measurements are limited to specific wavelengths, or a single phase angle. No measurements of combination of wavelengths and phase angles are available.
However combining the available measurements, models and knowledge a model can be constructed.
Bagnulo et al (2017) state the hypothesis that in the first order the polarization spectra may be expressed as a product of two functions, one that depends on phase angle, and one that only depends on wavelength.
Polarisation phase angle curves can be expressed by trigonometric functions (Lumme and Muinonen, 1993):

$P(\alpha) = b*(\sin(\alpha))^{c1}(\cos(\alpha/2))^{c2}\sin(\alpha - \alpha_{inv})$
With
P the polarization
α the phase angle
b the amplitude of the polarization
α_{inv} the inversion angle (the phase angle at which the polarization crosses the zero) ≈ 23°
c1 controls the position of the minimum ($\alpha_{min} \approx \alpha_{inv}/2$)
c2 affects the maximum and the asymmetry of the phase curve ($P_{max} \approx 105°$)
Values according Shkuratov et al (2015)

Polarisation wavelength function can be derived in first order from Umov law, which can be described as
$\text{Log}(A) = a(\log(P_{max})) + b$
With A the albedo (which here we need to derive from SCIAMACHY)
a = 0.724, b = -1.81 (at 600nm) according Dollfus and Bowell (1971)

The dependence of wavelength according Dollfus and Bowell (1971) equals
Log (P_max) = - 1.137 log (lambda) + 1.396 for the wavelengths they studied

The combination of these functions with the reflectance derived here will allow a simple lunar polarization model based on wavelength and phase angle. Given the unknown rotation of SCIAMACHY relative to the scatter plane, the polarization and rotation must be empirically determined, where we assume the polarization changes over wavelength as a function of the wavelength to a certain power, matching the work of Dullfus and Bowel:

$$\text{Polarisation} = P0 / \lambda^{P1},$$

with P0 (Degree of Polarisation) and P1 (Wavelength power-law index) empirically determined.

5.5 IMPROVED SCIAMACHY

From the improved SCIAMACHY measurements, updated measured lunar reflectances were derived as described in previous study. In summary: the lunar measurements were divided by the solar measurements and corrected for distances, the size of the slit, and scanning speed of the lunar observation. As in the previous study these measured lunar reflectances still contain some instrumental effects. In the previous study these were fitted as small linear multiplicative changes relative to an arbitrary reference geometry.
For this study we chose the reference geometry to be a (absolute) phase angle of 30° as this matches the geometry for which the RELAB measurement were performed (and all other geometries set to zero).
Additional tests showed (not shown here) that fitting in the exponential domain (instead of linear), similar as ROLO, results in smaller fitting residuals.

SCIAMACHY instrumental effects can thus be described as follows:

$$A\log(R_{measured}) = \log(R_{lunar}) + f(t) + f(ASM) + f(ESM) + f(ASM_{solar}) + f(polarization)$$

Where
f(t) is the degradation of the instrument, as third-order polynomial as function of time
f(ASM) is the second order dependence on the ASM mirror angle under which the moon was observed
f(ESM) is the first order dependence on the ESM mirror angle under which the moon was observed
f(ASM_solar) is the first order dependence on the ASM mirror angle under which the sun was observed
f(polarization) is the first order dependence of SCIAMACHY polarization dependence multiplied by the observed polarization.
The observed polarization however is strongly coupled to phase, and the polarization dependence on ASM angle. As expected and confirmed by the final results , the polarization terms capture the ASM dependence, and thus the ASM dependence was dropped from the final model (but is still mentioned here, due to its inclusion in the previous study).

However in order to fit these SCIAMACHY dependencies also the (true) lunar reflectance must be fitted at the same time. For the lunar model, see the next section.

6 PHASE B: IMPROVED LUNAR MODEL

6.1 IMPROVED LUNAR MODEL

A large variation of different lunar models were tested.
Dependences on various orders of lunar phase, both absolute and signed were tested, eg phase dependencies identical to Kieffer and Stone (2005) and Velikodsky et al (2011). Also all combination of the absolute phase or the square root of the absolute phase angle up till the 6th order were tested.
As expected higher order dependencies cause large unphysical behavior outside the range of measured phase angles (as observed with verification dataset). The addition of the square root of the absolute phase angle decreased the fitting residuals the most. As all other models 3 orders of phase angles were needed to accurately fit the measurements. In this case thus the square root of the phase, the absolute phase and the square root of the absolute phase to the power of 1.5. To avoid unphysical behavior outside the observed phase angle range the orders were kept as low as possible.
In addition to the phase angle, dependences on solar lunar longitude (1,2,3 and 5th order), libration latitude, libration longitude and all their cross-terms were tested. The cross-terms and higher orders did not improve the residuals, only increased fitting uncertainties (not shown here).
To describe the phase behavior at very small angle, similar to Kieffer and Stone (2005) two exponential terms were added dependent on absolute phase. Finally a cosine term was also clearly visible in the residuals and was thus added (similar Kieffer and Stone).

The best model to describe the measurements was found as the following
Alog(R_lunar) = f(sqrt(abs(lunar_phase))) + f(solar_longitude)+f(lunar_longitude) + f(lunar_latitude) + f(abs(lunar_phase)

Where
f(sqrt(abs(lunar_phase))) is a three order polynomial of the square root of the absolute value of the lunar phase angle [so g^0.5, g^1, g^1.5 and with g the absolute lunar phase angle], and f(solar_longitude), f(lunar_longitude) and f(lunar_latitude) the linear (first order) dependence on the observed libration longitude and latitude.
F(abs(lunar_phase)) equals P1*exp(-g*P2)+P3*exp(-g*P3)+P4*cos((g-P5)*P6). Note that these fitting parameters are inverted compared to Keiffer and Stone to avoid dividing by zero.

6.2 COMBINING LUNAR AND SCIAMACHY MODEL: SCIA+LUNAR MODEL

All measured SCIAMACHY lunar reflectances (which still contain instrument effects at this point) were fitted for the combined improved SCIAMACHY and lunar model

Alog(R_measured) = alog(R_lunar) + f(t) + f(ASM) + f(ESM) + f(ASM_solar) + f(polarization)
with the model for the lunar reflectance, R_lunar, given in section 6.1.
So

Alog(R_measured) = f(sqrt(abs(lunar_phase))) + f(solar_longitude)+f(lunar_longitude) + f(lunar_latitude) + f(abs(lunar_phase) + f(t) + f(ASM) + f(ESM) + f(ASM_solar)

This model was fitted iteratively to every wavelength independently for all geometries at once, discarding clear erroneous outliers. Note that the ASM dependence was fixed to zero (but mentioned here for historical reasons).
In order to improve the residuals the model was fitted in several steps:

First all SCIAMACHY instrument effects and the square root phase angle and solar longitude dependence (which together dominate the observed reflectance) were fitted. The found parameters were fixed and then the libration longitude and latitude were fitted. The found parameters were then fixed and then cosine term was fitted. The found parameters were then fixed and then first exponential term was fitted. The found parameters were then fixed and then second exponential term was fitted. The found parameters were then fixed and then the cosine term was refitted.
The found parameters were then fixed and then SCIAMACHY instrument effects, the square root phase angle, and solar longitude dependence were refitted. This multi-step approach was required due the very small impact of the various parameters. Due note that unlike Kieffer and Stone we were able to determine these parameters for all wavelengths, not a wavelength average.

The only parameter not determined in above steps was the polarization function as the polarization dependence is better determined as function of wavelength. After all wavelengths were fitted, the residuals of each measured spectrum were fitted to the calculated SCIAMACHY polarization dependence multiplied by an estimate of the observed polarization. As described by Dolfus and Bowel the polarization (maximum) decrease with wavelength (likely due to Umov effect). The observed polarization can thus be described by the observed reflectance to a certain (negative) order: so
(1+P1*mu2*polarization + P2*mu3*polarisation)
With the polarization parameterized as the polarization at 550nm with a power-law (P3) to the wavelength, so
Polarisation = Polarisation(550nm) * lambda^P[3]
The polarization at 550nm is fitted by P1 and P2.
Mu2 and Mu3 for each individual measurement is known from SCIAMACHY mirror model (Krijger et al 2014), allowing a fit to the polarization for each individual measurement. The fitted impact of polarization for each spectrum can be then divided out of R_lunar, removing thus the polarization from the signal.

In summary all parameters where fitted in the following order, with all non-mentioned parameters fixed (with their previous steps found value or zero if not derived yet):

- Phase angle & solar longitude
- Libration longitude & latitude
- Cosine Term
- First exponential
- Second exponential
- Cosine Term
- SCIAMACHY instrumental effects
- Polarisation

The resulting fitting residuals were smaller than in the previous study, and the noise in NIR/SWIR much reduced. Figure 14 shows the residuals from the fit to the SCIAMACHY measurements (instrumental and lunar effects). Overplotted in red is the polarization function (known SCIAMACHY polarization sensitivity multiplied with estimated degree polarization). The polarization spectral features are very clearly present. The shortest wavelength are less well represented, likely due to the large degradation at these wavelengths. The 350nm feature is sharped than the polarization function, because the moon does not fill the entire slit and thus does not cover the entire SCIAMACHY pixel width. It is know that the polarization feature is due a spatially limited contamination/damage to SCIAMACHY pixels that measure the 350nm wavelengths. The polarization sensitivity is measured for a fully illuminated slit, which is not the case for the lunar measurements. As such the 350nm feature is sharper for the lunar measurements than determined from on-ground measurements.
The longest wavelengths should not suffer from polarization. Their deviation is due to their larger intrinsic uncertainties. Note that the residuals are determined for each wavelength independently, while the polarization fit is determined for all wavelengths together.

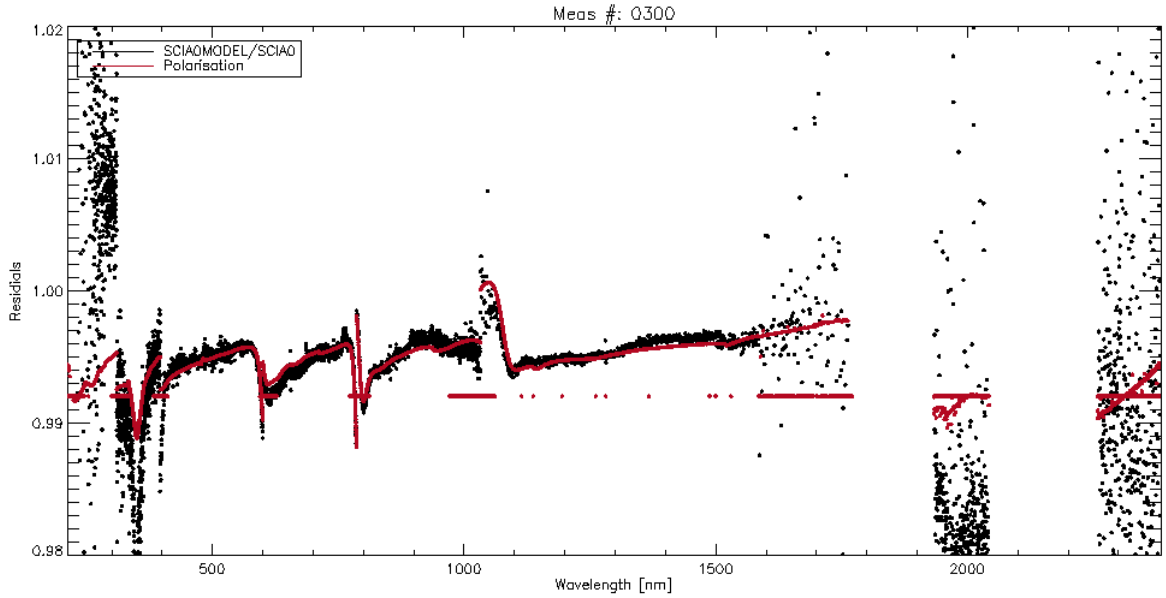

Figure 14 Relative residuals after instrumental fit (black) and following Polarisation fit to these residuals (red)

6.3 ONGROUND (RELAB) MEASUREMENTS

6.3.1 INTRODUCTION

For more information on the RELAB measurements, see:
http://www.planetary.brown.edu/relabdocs/LSCCsoil.html.

The RELAB measurements were obtained, downloaded, read and verified. A total of 20 materials are available with for each 4 different grainsizes, resulting in 80 different Relab spectra. All spectra were originally obtained with an illumination angle of 30 degrees at an observation angle of zero degrees (thus matching most a 30 degree phase angle) between 300 and 2600nm.

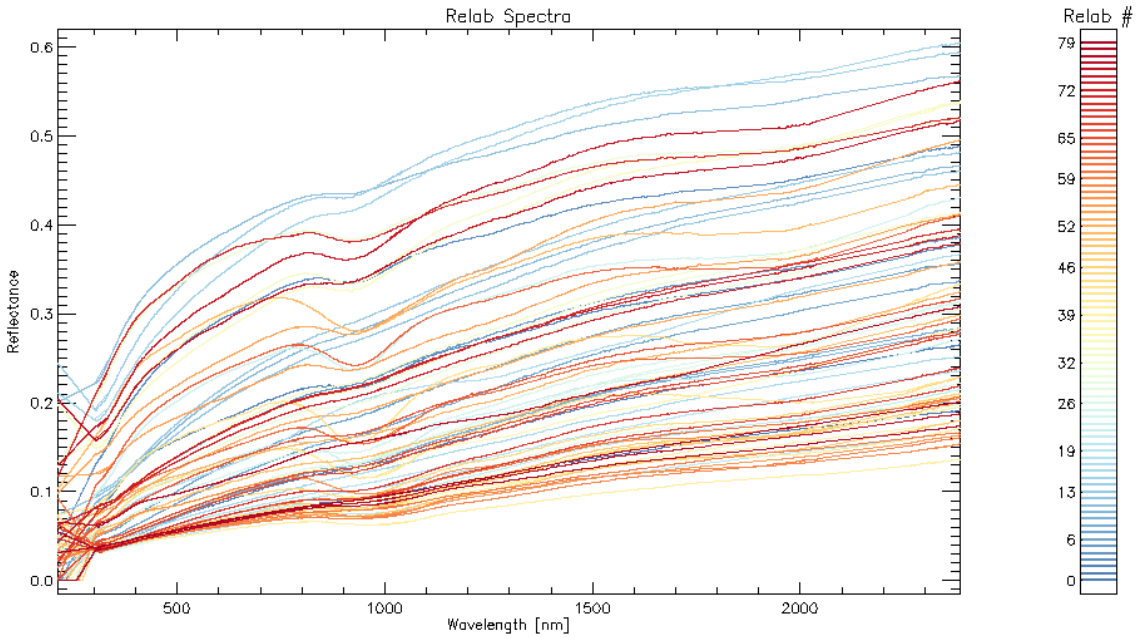

Figure 15 All 80 RELAB spectra

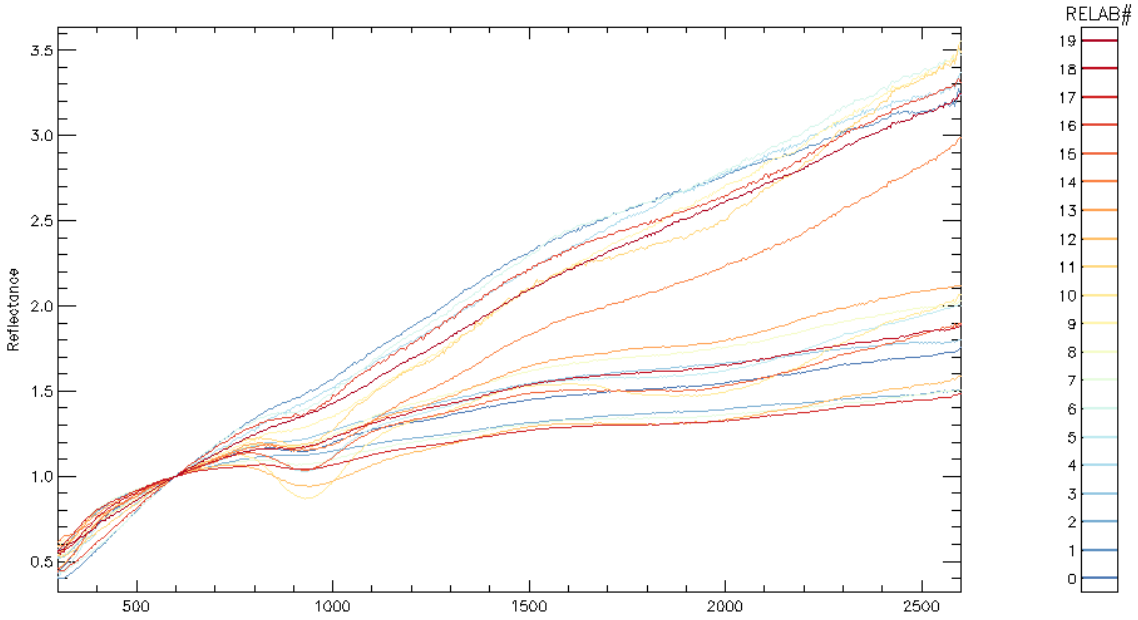

Figure 16 Selected RELAB lunar sample reflectance spectra (for grain sizes <450µm)

6.4 REFERENCE GEOMETRY LUNAR REFLECTANCE FIT (INTERMEZZO)

With 80 possible RELAB spectra to fit the observations, a solution is always found with the distribution weights of the different spectra dominated by local minima in the fitting process. As such the number of fitted spectra should be reduced. This will result in lower noise in the fit and allow studying the effect of various lunar geometries on the different weights of the spectra.
An iterative fitting method was thus created that removes spectra that contribute very minor (adjustable threshold) to any fit and then refits with the reduced spectra until all spectra contribute a (adjustable) minimal amount (here 0.3%). Note that all RELAB spectra are scaled to 600nm first to give them comparable weights.

Some RELAB spectra are very similar, such that for the fit there is no distinguishable difference and the fit fails (as the fit cannot decide between the two similar spectra). Some manual preselection of RELAB spectra is required. A more optimized pre-selection procedure has been been investigated, but the results were satisfactory (not shown here). An improved fitting algorithm employing the Levenberg-Marquardt technique (instead of multiple linear regression) was thus developed. The new fitting algorithm can handle the (similar) employed RELAB spectra without manual preselection.

The reference (30 degree phase) SCIAMACHY measurement (so without instrumental effects) was fitted successfully to the RELAB spectra. Included wavelengths for the fit are indicated in red. Note that the higher wavelengths (which will be corrected for BRDF later) have not been included in the fit, but still result in reasonable (for SCIAMACHY standards) match. The RELAB spectra have no information below 300nm and are an extrapolation, which is clearly wrong.

This result confirms that the moon surface consists of various combinations of moondust.

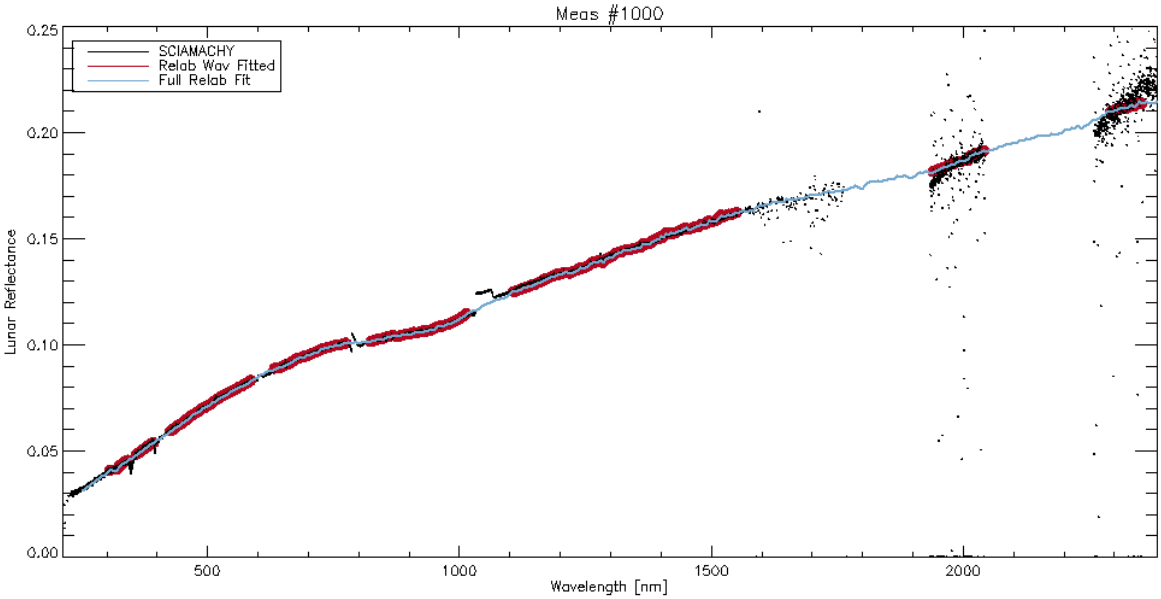

Figure 17 Comparison between SCIAMACHY and RELAB fits for a representative measurement. Red areas are the wavelenghts employed in the RELAB fit (blue).

6.4.1 GRAIN SIZE

For this study we selected only those spectra which were the least sifted and contain the coarsest grains (<450µm). Extensive testing to vary the number of RELAB spectra, including all grain sizes, specific grainsizes, random grainsizes, and optimized grainsizes were performed. No significant improvements were found, only the uncertainty per fitted RELAB spectra increased (as the number of parameters increased). As such the remainder of this study restricts itself to coarsest grain spectra of each measured RELAB material. This is confirmed by the work of Taylor (2001) which has shown that the lunar reflectance is dominant by these coarsest grains. Note that all RELAB spectra are scaled to 600nm first to give them comparable weights.

6.5 COMBINING SCIAMACHY & RELAB

Having found that the reference lunar reflectance could be described by a linear combination of RELAB spectra, an investigation was performed to describe all lunar reflectances (after instrumental effect removal) with RELAB spectra.
For each SCIAMACHY measured, the fitted lunar+SCIAMACHY instrumental model was split in a derived lunar reflectance and an instrumental effects part. This can be done technically by setting the fitting parameters to zero, eg for the SCIAMACHY part all lunar reflectance weights are set to zero. As we are here interested in the lunar part, and not the SCIAMACHY instrumental effect, the lunar part was derived by dividing out the SCIAMACHY instrumental part.
The resulting derived lunar reflectance is considered to describe the lunar reflectance for the observed geometry.

Each (for a single geometry) derived lunar reflectance spectra is then fitted individually with a linear combination of RELAB spectra. The weights of the overlap regions and the 350nm polarization feature were set to zero as not to impact the broadband fit. The weights were equally distributed across observed wavelengths to avoid the lower wavelengths from dominating the fit.
The resulting fitting residuals (not shown here) are slightly smaller than the estimated uncertainty of the derived lunar reflectances by the SCIAMACHY+lunar model and thus improve the signal to noise ratio. Note that no information on lunar geometry is employed in this step.

So
R_lunar_relab = f(RELAB, R_lunar)
Where f(RELAB) is a linear combination of RELAB spectra fitted to R_lunar

Yet RELAB spectra have no measurements below 300nm and the RELAB measurement at 300nm is also very noisy. SCIAMACHY however has reliable measurements down to about 250nm! Therefor the fitted RELAB spectra to the derived lunar reflectance (R_lunar_relab) are extended with a linear fit to the SCIAMACHY lunar reflectance measurements between 250 and 300nm. Alternatives to a linear fit have been investigated but did not improve results. The SCIAMACHY extension to the RELAB fit seem to behave very similarly (not shown here).

As the RELAB spectra are measured at a 5nm grid the derived lunar reflectances are also on this lower resolution grid. SCIAMACHY measurements indicate no structures smaller that 50nm exist in the lunar spectra and thus this reduction in spectral resolution results in no loss in information (verified, not shown here). If higher spectral resolution is required, the spectra at 5nm resolution can simply be interpolated (if the correct units (per nm) are employed).

The advantage of this approach is that any remaining spectral structures (either from residual instrument effects or fitting uncertainties) are removed. It also provides lunar spectra for the full 300 to 2500nm range instead of only the wavelengths measured by SCIAMACHY, which has large gaps in the NIR/SWIR region and erroneously behaving smaller overlaps between channels.

6.6 NEW MODEL DESCRIPTION: LESSSR

Having now Lunar reflectances consisting of a linear mix of RELAB spectra, and slightly extended to 250nm (R_lunar_relab), which are much more spectrally smooth and without SCIAMACHY instrumental effects, the lunar model is again fitted to these derived lunar reflectances at the full 5nm between 250-2500nm grid and not just the SCIAMACHY wavelengths:

The fits are done identical as in the previous step when fitting SCIAMACHY instrumental effects (in the various steps of phase, libration, cosine, exponential), only now all SCIAMACHY dependencies are fixed to zero.

This results in a lunar model dependent only on lunar phase, lunar solar longitude, libration longitude and latitude at a 5nm spectral grid between 250 and 2500nm.

The model values are provided separately from this document. The model describes the lunar reflectances for each wavelength as follows:

$$Alog(R\_lunar) = P0 + P1\, g^{0.5} + P2\, g + P3\, g^{1.5} + P4\, \Phi + P5\, \phi + P6\, \theta + P7 \cdot \exp(-g \cdot P8) + P9 \cdot \exp(-g \cdot P10) + P11 \cdot \cos((g - P12) \cdot P13).$$

With g the absolute lunar phase, ϕ and θ the selenographic longitude and latitude of the observer, and $\Phi + P5$ the selenographic longitude of the Sun.

The proposed name for this model is the LESSSR (**L**unar **E**xtended **S**atellite **S**imulation **S**olar **R**eflectance) model. The **E** can also refer to EUMETSAT or European.

7 PHASE C: MODEL VALIDATION

7.1 COMPARISION WITH SCIAMACHY MEASUREMENTS

Figure 18 shows for all measurements at 550nm the residuals as function of phase angle. In yellow the residuals between the SCIAMACHY measurement (SCIA0) and the model describing the SCIAMACHY measurement (SCIA0MODEL) employing both lunar and instrument features. This instrument and lunar model then has all instrumental effects removed resulting in a lunar reflectance as measured by a SCIAMACHY without instrument effects (SCIA). To this corrected lunar reflectance spectrum (SCIA) the RELAB measurements are fitted. The residuals between the estimated lunar reflectance (SCIA) and the RELAB fit (RELAB) is shown in red. These lunar geometry independent RELAB fits are then modelled as function of lunar geometries by the LESSSR model. The residuals between the RELAB fits and the LESSSR model are shown in black. The total residual between the estimated lunar reflectances (SCIA) and the LESSSR model is shown in blue. For 550 nm the residuals are dominated by the instrumental uncertainties (SCIA0MODEL/SCIA0). Later steps have residuals smaller than 0.2%. Other wavelengths show similar results, eg 1550nm is visible in Figure 19.

Figure 20 shows a sample measured lunar reflectance (after instrumental effects removal) in blue and the RELAB fit in black and the final LESSR model in red. In the SCIAMACHY measurements some noise at the higher wavelengths is still visible, as all measurements are shown here for comparison. In the fitting procedure these noisy pixels are given a weight of zero and thus not taken into account. This visual comparison shows that the SCIAMACHY channel edges have some issues remaining due to limited knowledge of polarization sensitivity (determined on-ground). As such these edges have not been given any weight in the model fits.

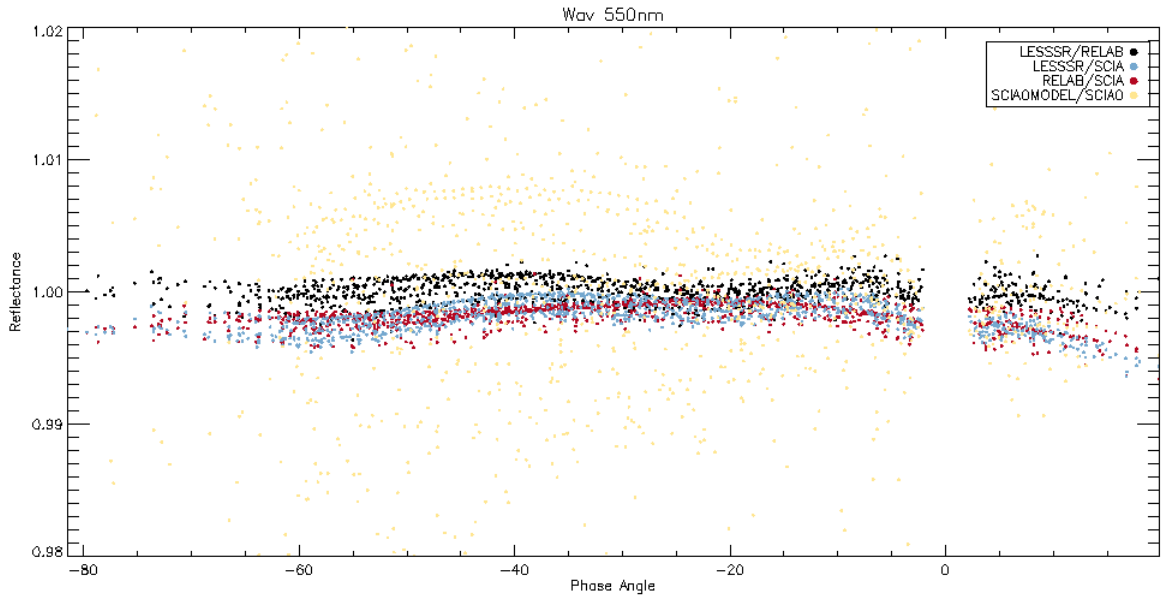

Figure 18 Residuals of all fitting steps for 550nm

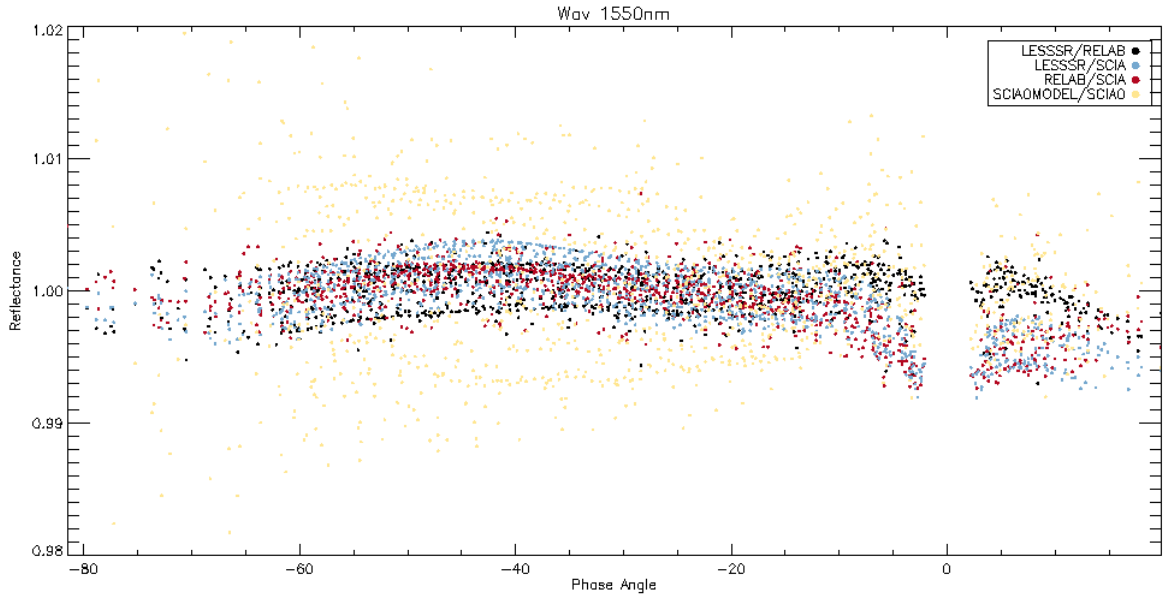

Figure 19 Residuals of all fitting steps for 1550nm

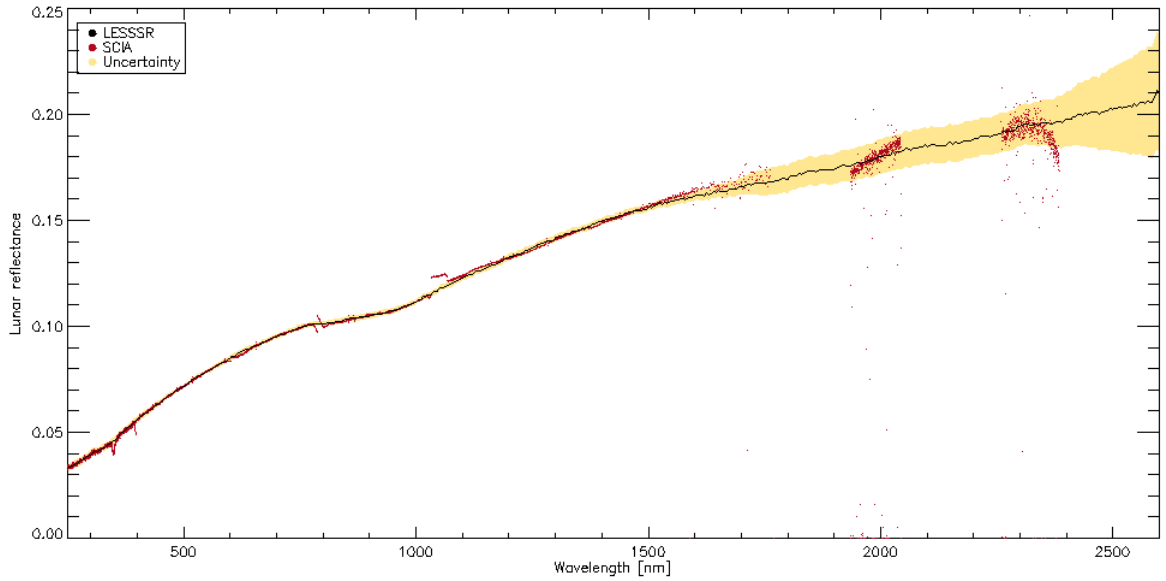

Figure 20 Sample lunar reflectance and its model uncertainty

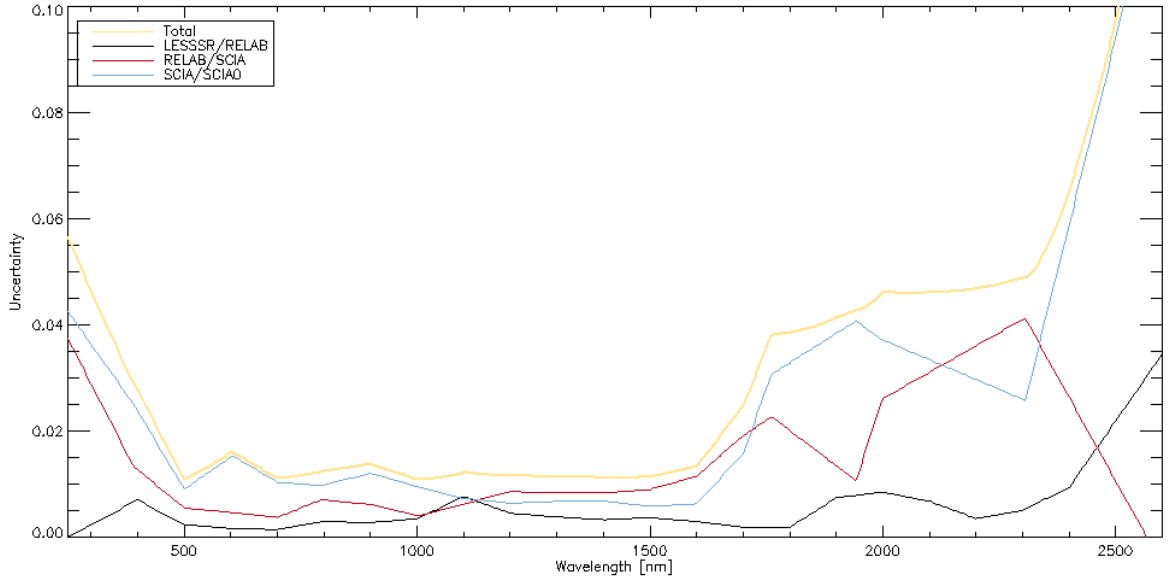

Figure 21 LESSSR and sub models relative (to reflectance) uncertainties. A 0.01 uncertainty is thus 1% uncertainty on the reported reflectance.

7.2 COMPARISON WITH GOME2 MEASUREMENTS

Figure 22 shows the comparison between LESSSR model and the model derived from GOME2. As the two models have no overlapping measurements, a reference geometry at 65 degrees phase angle and all other geometry dependencies set to zero degrees is compared. LESSSR is slightly larger at the lower wavelengths, but this is likely due to the (strong) degradation that GOME2 suffers from. The GOME2 measurements are only degradation corrected from the first measurement, while it is known the degradation must already have started before the first measurement. The order of magnitude and relative smooth wavelength behavior support this hypothesis.

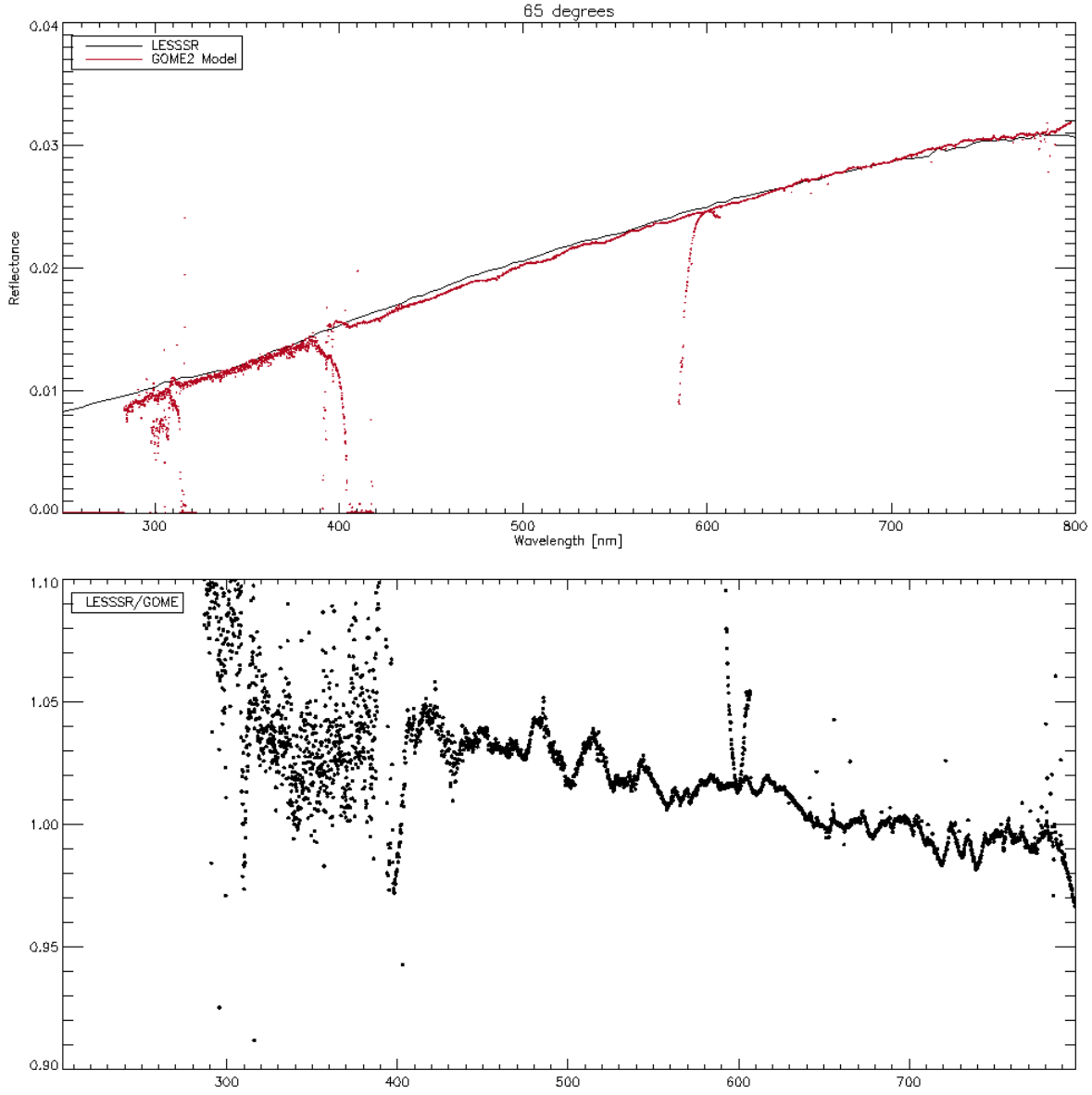

Figure 22 Top: Absolute comparison between reference geometry at 65 degrees phase angle for LESSSR and GOME2. Bottom relative comparison

7.3 COMPARISON WITH GIRO SIMULATED MEASUREMENTS

Figure 23 shows the lunar reflectances as provided by GIRO relative to those provided by LESSSR as function of phase angle. The difference can be several percent large. Which of the two is the better is hard to estimate from a direct comparison.

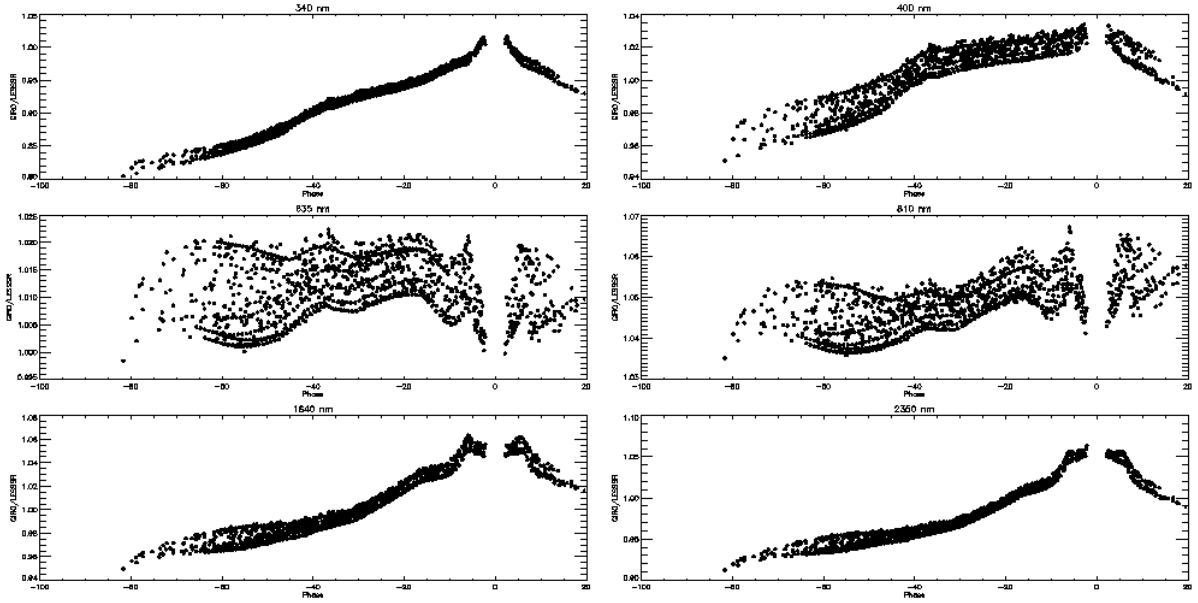

Figure 23 Comparison LESSSR/GIRO

7.4 COMPARISON WITH SEVIRI MEASUREMENTS

Figure 24 shows the bias between SEVIRI measurements and LESSSR (black), and the bias between SEVIRI measurements and GIRO (red) as function of phase angle, with the black line as the median of the LESSSR ratio.

Note how at the 1640nm channel LESSSR does not have the phase angle dependence that GIRO has. The absolute level seems to change as function of wavelength (note that at 635nm the LESSSR ratio is closer to one), it is unknown if this is due either both GIRO and LESSSR or SEVIRI having a wrong calibration.

Figure 25 shows the same biases but for the full range of the SEVIRI measurements. Measurements outside the GIRO valid geometry range have been set to 1. As expected LESSSR should likely not be used outside of its validity range (-90 to about 20 degree phase), as for higher phase angles a slight (few percent) phase dependence can be seen when compared to SEVIRI.

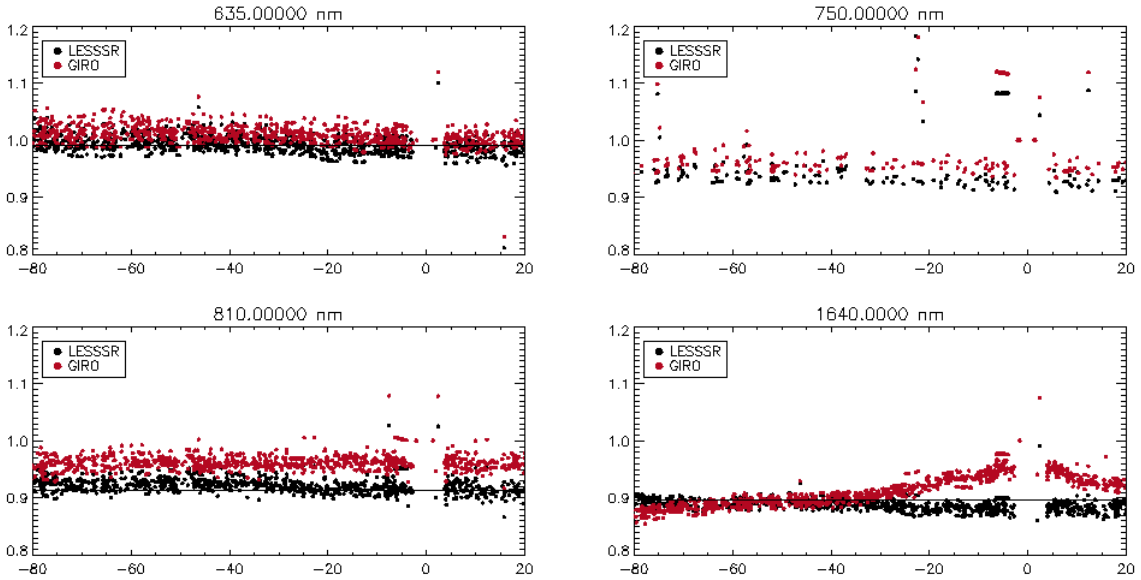

Figure 24 SEVIRI comparison with LESSR and GIRO for SCIAMACHY geometry range

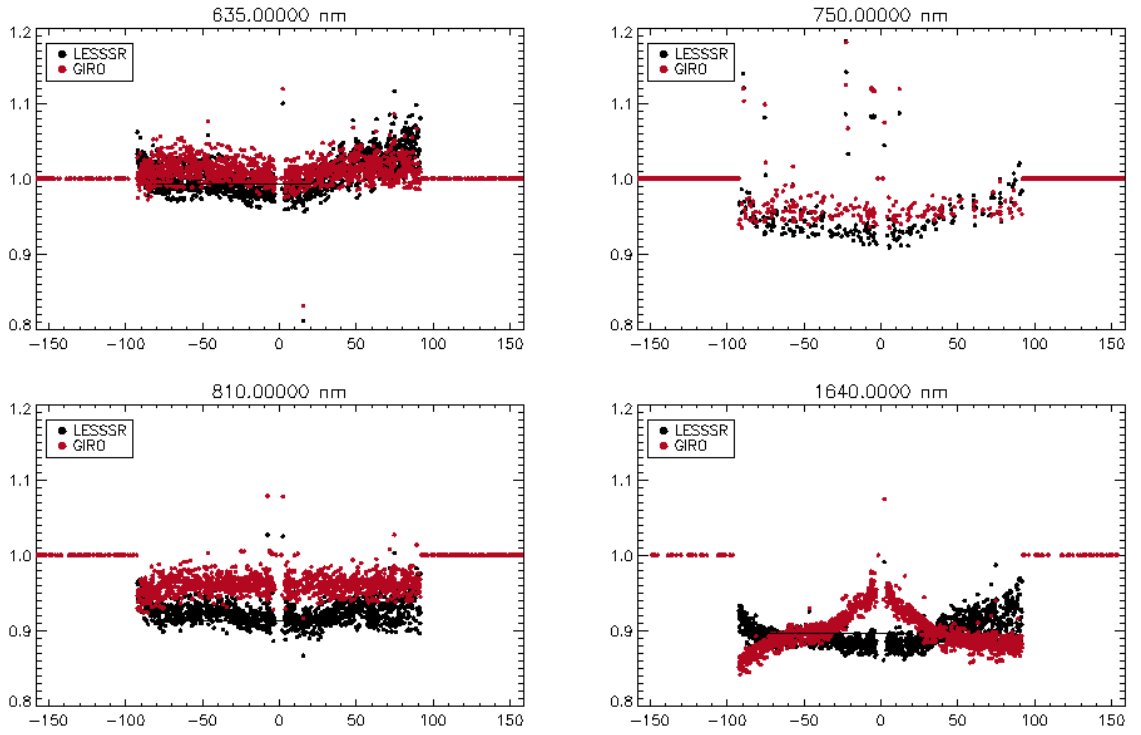

Figure 25 SEVIRI comparison with LESSR and GIRO full geometry range

8 PHASE D: ABSOLUTE REFLECTANCE

GOME2 is measured around -50 degrees solar longitude, while SCIAMACHY is measured between -20 and 80 degrees solar longitude. As can be seen in Figure 26 LESSSR (black) does not observe any higher order dependence on solar longitude, while GIRO (black) does. Given this disagreement between LESSSR and GIRO and the non-overlapping geometries between SCIAMACHY and GOME2 measurements (Figure 5) and hints of initial GOME2 degradation (Figure 22), we do not suggest at this point to recalibrate the LESSSR model with the GOME2 absolute calibration as was considered an option during proposal.

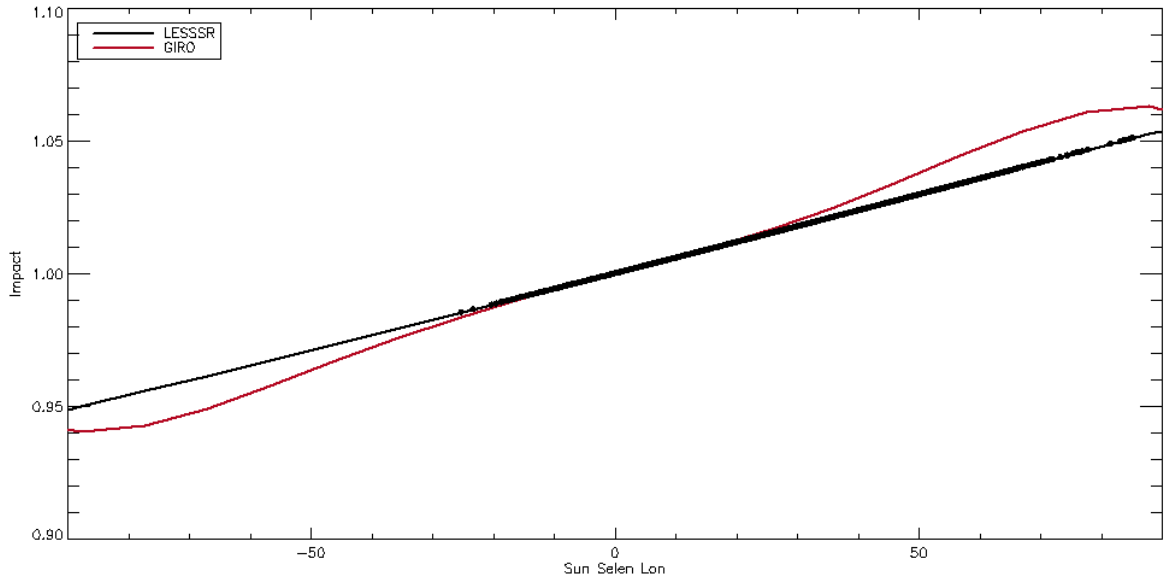

Figure 26 Impact of Solar Longiture for 550nm according GIRO and LESSSR. GOME2 is measured around -50 degrees, while SCIAMACHY is measured between -20 and 80 degrees. LESSSR does not observe the higher order dependence

9 CONCLUSION

This document describes a study on the characterisation of the reddening effect on the lunar reflectance spectrum of varying illumination conditions and the comparison with the current GIRO mechanism accounting for this effect.
We presented an updated lunar reflectance model named LESSSR (Lunar ESS SCIAMACHY RELAB), validated by GOME2 and SEVIRI measurements. The model employs a combination of in-flight SCIAMACHY measurements and on ground RELAB measurements and improves on previous (SCIAMACHY) lunar models (due to inclusion of polarization and noise reduction) and GIRO (which shows phase dependence on SWIR wavelengths when compared to other measurements).
The outcome of this study allows a better understanding of the phase dependence observed with some satellite datasets, such as the Meteosat lunar data acquired with the SEVIRI instruments, which cover GIRO's full range of illumination conditions.
The LESSSR model describes the disk-equivalent lunar reflectance (R_lunar) as follows at a grid of 5nm between 300nm and 2500nm:

Alog(R_lunar)= P0+P1 *g*^0.5 + P2 *g*+P3 *g*^1.5 + P4 Φ + P5 ϕ + P6 θ
+ P7*exp(-g*P8)+P9*exp(-g*P10)+P11*cos((g-P12)*P13).

With *g* the absolute lunar phase, ϕ and θ the selenographic longitude and latitude of the observer, and Φ + P5 the selenographic longitude of the Sun.

The LESSSR model based upon SCIAMACHY measurements seem to improve on the GIRO model when comparing to SEVIRI.

10 REFERENCES

- Dobber, Marcel R.; Goede, Albert P. H.; Burrows, John P., 1998, Observations of the Moon by the Global Ozone Monitoring Experiment: Radiometric Calibration and Lunar Albedo, Applied Optics LP, vol. 37, Issue 33, pp.7832-7841, DOI: 10.1364/AO.37.007832
- Krijger, J. M., Snel, R., van Harten, G., Rietjens, J. H. H., and Aben, I. , 2014., Mirror contamination in space I: mirror modelling, Atmospheric Measurement Techniques, 7, 3387–3398, doi: 10.5194/amt-7-3387-2014, http://www.atmos-meas-tech.net/7/3387/2014/
- Hilbig, T., Weber, M., Bramstedt, K. et al. Sol Phys (2018) 293: 121. https://doi.org/10.1007/s11207-018-1339-9
- Liebing, Patricia & Krijger, J.M. & Snel, Ralph & Bramstedt, Klaus & Noël, Stefan & Bovensmann, Heinrich & P. Burrows, John. (2018). In-flight calibration of SCIAMACHY's polarization sensitivity. Atmospheric Measurement Techniques. 11. 265-289. 10.5194/amt-11-265-2018.
- NASA Reflectance Experiment Laboratory (RELAB) http://www.planetary.brown.edu/relabdocs/relab.htm
- Earth Space Solutions Study report for EUMETSAT: Validation of Spectral Band Adjustment Factors using Lunar Hyperspectral Measurements, Activity 1 & 2, 07.06.2017, *ESS-LUN-RP-001-Rev4*
- Earth Space Solutions Study report for EUMETSAT: Validation of Spectral Band Adjustment Factors using Lunar Hyperspectral Measurements, Activity 3, 07.06.2017, *ESS-LUN-RP-003-Rev3*
- Earth Space Solutions Study report for EUMETSAT: Validation of Spectral Band Adjustment Factors using Lunar Hyperspectral Measurements, Activity 4, 05.10.2017, *ESS-LUN-RP-004-Rev1*
- Kieffer, H., H., Stone, T. C The Spectral Irradiance of the Moon, *2005, The Astronomical Journal, 129,2887*

- Lipskii, Yu. N. and Pospergelis, M. M., "Some Results of Measurements of the Total Stokes Vector for Details of the Lunar Surface.", 1967
- Escobar-Cerezo, J., Muñoz, O., Moreno, F., Guirado, D., Gómez Martín, J. C., Goguen, J. D., Garboczi, E. J., Chiaramonti, A. N., Lafarge, T., and West, R. A., "An Experimental Scattering Matrix for Lunar Regolith Simulant JSC-1A at Visible Wavelengths", 2018, DOI: 10.3847/1538-4365/aaa6cc
- Shkuratov, Iu. G. and Opanasenko, N. V., "Polarimetric and photometric properties of the moon: Telescope observation and laboratory simulation 2. The positive polarization", 1992, DOI: 10.1016/0019-1035(92)90161-Y
- Dollfus, A. and Titulaer, C., "Polarimetric Properties of the Lunar Surface and its Interpretation. Part III", 1971, DOI:
- Dollfus, A., Geake, J. E., and Titulaer, C., "Polarimetric properties of the lunar surface and its interpretation. Part 3: Apollo 11 and Apollo 12 lunar samples", 1971, DOI:
- Bagnulo, S., Belskaya, I., Cellino, A., and Kolokolova, L., "Polarimetry of small bodies and satellites of our Solar System", 2017, DOI: 10.1140/epjp/i2017-11690-6
- Shkuratov, Yuriy, Opanasenko, Nikolay, Korokhin, Viktor, and Videen, Gorden, "The Moon", 2015, DOI:
- Shkuratov, Y., Kaydash, V., Korokhin, V., Velikodsky, Y., Opanasenko, N., and Videen, G., "Optical measurements of the Moon as a tool to study its surface", 2011, DOI: 10.1016/j.pss.2011.06.011
- Zubko, Evgenij, Videen, Gorden, Zubko, Nataliya, and Shkuratov, Yuriy, "Reflectance of micron-sized dust particles retrieved with the Umov law", 2017, DOI: 10.1016/j.jqsrt.2017.01.003
- Dollfus, A., Bowell, E., and Titulaer, C., "Polarimetric Properties of the Lunar Surface and its Interpretation. Part II. Terrestrial Samples in Orange Light", 1971, DOI:
- Wolff, M., "Theory and application of the polarization-albedo rules", 1980, DOI: 10.1016/0019-1035(80)90144-X

- Grynko, Y., Shkuratov, Y.G., “Light scattering from particulate surfaces in geometrical optics approximation” In: Kokhanovsky A.A. (eds) Light Scattering Reviews 3. Springer Praxis Books. Springer, Berlin, Heidelberg, 2008, DOI:10.1007/978-3-540-48546-9_9
- ((Grynko Y., Shkuratov Y.G. (2008) Light scattering from particulate surfaces in geometrical optics approximation. In: Kokhanovsky A.A. (eds) Light Scattering Reviews 3. Springer Praxis Books. Springer, Berlin, Heidelberg))
- Zubko, Nataliya, Gritsevich, Maria, Zubko, Evgenij, Hakala, Teemu, and Peltoniemi, Jouni I., "Optical measurements of chemically heterogeneous particulate surfaces", 2016, DOI: 10.1016/j.jqsrt.2015.12.010
- Munoz, O., Moreno, R., Guirado, D., Dabowska, D. D., Volten, H., and Hovenier, J. W., "The Amsterdam-Granada Light Scattering Database.", 2012, DOI:
- Holsclaw, G. M., Snow, M., and McClintock, W. E., "Disk-integrated Polarization of the Moon in the Ultraviolet", 2012, DOI:
- Shkuratov, Yuriy, Zubko, Evgenij, and Videen, Gorden, "Interpreting lunar polarimetric anomalies at large phase angles", 2017, DOI: 10.1016/j.icarus.2017.05.023
- Shkuratov, Y., Kaydash, V., Korokhin, V., Velikodsky, Y., Petrov, D., Zubko, E., Stankevich, D., and Videen, G., "A critical assessment of the Hapke photometric model", 2012, DOI: 10.1016/j.jqsrt.2012.04.010
- Shkuratov, Yu., Opanasenko, N., Opanasenko, A., Zubko, E., Bondarenko, S., Kaydash, V., Videen, G., Velikodsky, Yu., and Korokhin, V., "Polarimetric mapping of the Moon at a phase angle near the polarization minimum", 2008, DOI: 10.1016/j.icarus.2008.06.014
- Dollfus, A. and Bowell, E., "Polarimetric Properties of the Lunar Surface and its Interpretation. Part I. Telescopic Observations", 1971, DOI:
- Shkuratov, Yu & Videen, Gorden & Kreslavsky, Mikhail & Belskaya, Irina & Kaydash, Vadym & Ovcharenko, A & Omelchenko, V & Opanasenko, Nikolay & Zubko, Evgenij. (2005). Scattering Properties of Planetary Regoliths Near Opposition. 10.1007/1-4020-2368-5_8. In Morozhenko, Alexander & Vidmachenko, A. (2005). Polarimetry and Physics of Solar System Bodies. Photopolarimetry in Remote Sensing, NATO Science Series II: Mathematics, Physics and Chemistry. 161. 369-384. 10.1007/1-4020-2368-5.
- Pieters, C. M., "The Moon as a Spectral Calibration Standard Enabled by Lunar Samples: The Clementine Example", 1999, DOI:
- Taylor, Lawrence A., Pieters, Carlé M., Keller, Lindsay P., Morris, Richard V., and McKay, David S., "Lunar mare soils: Space weathering and the major effects of surface-correlated nanophase Fe", 2001, DOI: 10.1029/2000JE001402
- Lawrence, S. J., Lau, E., Steutel, D., Stopar, J. D., Wilcox, B. B., and Lucey, P. G., "A New Measurement of the Absolute Spectral Reflectance of the Moon", 2003, DOI:
- Pieters, C. M., Taylor, L. A., McKay, D., Wentworth, S., Morris, R., and Keller, L., "Spectral Characterization of Lunar Mare Soils", 2000, DOI:
- Fearnside, Andrew, Masding, Philip, and Hooker, Chris, "Polarimetry of moonlight: A new method for determining the refractive index of the lunar regolith", 2016, DOI: 10.1016/j.icarus.2015.11.038
- Hapke, B., "The Refractive Index of the Regolith of Mercury", 1994, DOI:
- Gehrels, T., Coffeen, T., and Owings, D., "Wavelength dependance of polarization. III. The lunar surface.", 1964, DOI: 10.1086/109359
- Shkuratov, Iu. G. and Opanasenko, N. V., "Polarimetric and photometric properties of the moon: Telescope observation and laboratory simulation 2. The positive polarization", 1992, DOI: 10.1016/0019-1035(92)90161-Y